Full Paper

Structural Aspects and Thermal Properties of the Solid Fast Ionic Conductor [xCuI:(1-x)Ag$_2$CdI$_4$] (x = 0.2, 0.4, 0.6 and 0.8 mol. Wt %)

Noorussaba and Afaq Ahmad[*]

Department of Chemistry, Aligarh Muslim University, Aligarh- 202002, India

*Corresponding Author, Tel.:+91-94 119 83056; Fax: +91-85 330 86151

E-Mails: afaqahmad21@gmail.com

Abstract- The [xCuI:(1-x)Ag$_2$CdI$_4$] fast ionic conductors with various compositions corresponding to x=0.2, 0.4, 0.6 and 0.8 mol. wt % have been prepared by solid state reaction. The fast ionic conductors are characterized by X-ray powder diffraction, FTIR, DTA, DSC, TGA studies. The transmittance spectra of the fast ionic conductors [xCuI:(1-x)Ag$_2$CdI$_4$] (x=0.2, 0.4, 0.6 and 0.8 mol. wt. %) have been measured in the mid-infrared range to investigate the structure of the cadmium iodate anion [(CdI$_4$)$^{2-}$] matrix and the nature of sites hosting the charge carrier copper ions. X-ray powder diffraction, DTA, DSC, TGA studies was also carried out for confirming doping effect in the formation of composite in which the interface layer plays an important role in controlling the bulk properties of the material.

Keywords- X-ray diffraction, FTIR analysis, Thermal analysis, Doping, Fast ion conductors

1. INTRODUCTION

Solid fast ionic conductors have been the focus of interest in recent years due to their well known applications. A great deal of attentions has been paid more recently to enhance the conductivity of solid electrolytes [1]. Ag$_2$CdI$_4$ compound belongs to the so called superionic materials of A$_2$BI$_4$ type (A=Cu, Ag, In, B=Hg, Cd, Zn), that undergoes phase transition into

superionic state [2]. Ag_2CdI_4 compound possess smeared phase transition into the superionic state in the temperature region 330-380K. The solid fast ion conductor Ag_2CdI_4 exhibits a number of solid state phase transitions upon heating. Room temperature, covalent phase Ag_2CdI_4 crystallizes in a well-defined, structure. Ag_2CdI_4 at T<330 K belongs predominantly to hexagonal, β-Ag_2CdI_4 with space group P6/mmm and unit cell dimensions a=4.578 and c=7.529Å and changes to cubic at T>380 K with space group Pm3m and unit cell dimension a=5.05 Å [3].

AgI containing conductors have been extensively investigated as model fast ionic conductors because of their high ionic conductivity at room temperature (in the range of 10^{-1} to 10^0 Sm^{-1}). In recent years, new superionic glass compositions were prepared as a Cu^+ conducting glasses [4-9]. Such Cu^+ ion conducting composites exhibits conductivities which are comparable, or ever higher in some cases than the conductivities of the known silver analogues. However only a few works have been reported so far on the structural aspects of the new Cu^+ ion conductors in conductors in comparision to the widely investigated Ag^+ containing conductors [4].

In many cases it has been observed that the sequence of conductivity of conductors containing Ag^+, Li^+ or Na^+ ions is

$$\sigma_{(Ag^+)} \quad > \quad \sigma_{(Li^+)} \quad > \quad \sigma_{(Na^+)} \tag{1}$$

where $\sigma_{(M^+)}$ stands for the conductivity of conductors containing M^+ ions with the ionic radius taken into account, the above sequence (1) cannot easily be explained. The ionic radius of Ag^+, Cu^+, Li^+ and Na^+ are listed in Table 1, together with the electronic configuration of these ions. The radius of Ag^+ ionic radius values, the conductivity sequence (1) above is well established.

Table 1. Ionic radius and electronic configuration of some monovalent cations

Sample	Radii/pm	Configuration	Configuration of Lewis Acids
Ag^+	126	[Kr core] $4d^{10}$	Soft
Cu^+	96	[Ar core] $4d^{10}$	Soft
Li^+	68	[He core] $4d^{10}$	hard
Na^+	97	[Ne core] $4d^{10}$	hard

On the other hand, Li^+ and Na^+ ions have the s^2 and s^2p^6 configuration (rare gas type) in the outermost orbitals, while Ag^+ ions have the complete d^{10} configuration, and thus Li^+ and Na^+ ions are classified as hard Lewis acids, but Ag^+ ions as a soft Lewis acids [10].

We have postulated that such a difference of electronic configuration of ions, as well as the radius, affects the ions transport and therefore affects the conductivity of glasses [11,12]. Since Cu^+ ions have a similar d^{10} configuration and a smaller radius than that of Ag^+ ions. Glasses containing Cu^+ ions may be expected to exhibit high conductivities than those of glasses containing Ag^+ ions. Sudarshan et al. [13,14] studies the IR and Raman Spectra of this compounds. Bolesta et al, [15] calculated the band structure of Ag_2CdI_4 by semi-empirical method using strong band approximation. Yunakova et al. [16], studied the temperature dependence of the spectral positions and half-width of the A band in the range 90-430K in Ag_2CdI_4. Nair et al [17] studied the behaviour of Ag^+ in Ag_2CdI_4 by cation substituted smaller Li^+ and the larger Tl^+ ions. Kalid et al [2] studied the K^+ doping in Ag_2CdI_4. Inspire by the results we have tried to prepare Ag_2CdI_4 and study the effect of Cu^+ substitution on the structural effect and conductivity.

2. EXPERIMENTAL

2.1. Material

The following materials were used as received; cadmium [II] iodide and silver iodide were of Loba Chemie and CDH anal grade (India), each of which had a purity of 99.2%, 99% respectively.

2.2. Preparation and characterization of pure and doped samples

2.2.1. Preparation of pure [Ag₂CdI₄] host sample

Pure silver tetra iodocadmiate (Ag_2CdI_4) was prepared from stoichiometric amounts of CdI_2 and AgI by the solid state reaction method. AgI and CdI_2 were mixed in the requisite composition in 1:2 molar ratios, in an agate mortar (each above 300-mesh size). The finely ground stoichiometric mixture of the binary components AgI and CdI_2; was sealed in a glass ampoule and was placed in an air oven (CE 0434 NSW-144) at 150°C (423K) for 5 days (120 hrs) with intermittent grinding. The rate of heating was initially kept at 50°C per hours for 12 h. A light lemony yellow color compound was formed which changed to dark lemony yellow on cooling, Ag_2CdI_4 is dark lemony yellow above 57-107°C [2]. X-ray diffraction studies showed this light lemony yellow color compound to be single phase β-Ag_2CdI_4. The formation of the compounds was verified using x-ray diffractogram [18,19]

2.2.2. Preparation of doped sample [xCuI:(1-x)Ag₂CdI₄]

Cu^+ ion doped composite fast ion conductors were prepared by adding CuI to the host, Ag_2CdI_4. [xCuI:(1-x)Ag₂CdI₄] solid solutions was prepared by mixing 0.8,0.6,0.4 and 0.2 mol. wt.% Ag_2CdI_4 and x = 0.2,0.4,0.6 and 0.8 mol. wt.% CuI respectively, in an agate

mortar at room temperature with intermittent grinding adopting the procedure reported earlier [20]. The powder mixture, were ground thoroughly in an agate mortar and collected in a silica crucible which is then kept in an air oven (CE 0434 NSW- 144) for 24 hours at 150ºC. The resulting material at room temperature was used for further studies [21].

2.3. Characterization of pure and doped samples

2.3.1. X-ray powder diffraction

The x-ray diffraction studies were performed for the pure hosts [Ag_2CdI_4] and the mixed composite systems [$xCuI:(1-x)Ag_2CdI_4$] after the reaction was completed using Rigaku-D/Max-B diffractometer with a K-beta filter with CuKα (λ=1.5406 Å) radiation at room temperature. The angle range for measurement was 10–70° and the scanning speed was 1°/min. X-ray diffraction patterns suggest the formation of the pure Ag_2CdI_4 and doped [$xCuI:(1-x)Ag_2CdI_4$] samples.

2.3.2. FTIR measurements

The IR spectrum was recorded for the pure Ag_2CdI_4 and [$xCuI:(1-x)Ag_2CdI_4$] mixed composite systems in the mid-infrared range 400-4000 Cm^{-1} (25-25 μm) at room temperature using a INTERSPEC 2020, FTIR spectrophotometer measured in KBr.

2.3.3. Thermal analysis

Thermal characterization was carried out on pure Ag_2CdI_4 and [$xCuI:(1-x)Ag_2CdI_4$] mixed composite samples, using a universal $V_{2.6}$ D differential Scanning Calorimetry (DSC) TA-2010 instrument equipped with disk memory and data analyzer in the temperature range 20°C-400°C, with the powder sample sealed in pt capsules at heating rates of 10 K min^{-1}/air medium. Temperature calibration was prepared using a standard 'In' sample. Before carryings out the DSC, the samples was dried in a vacuumed oven for an hour at 100°C and then cooled down to room temperature, thereafter sample was equilibrated at 20°C for 10 min.

3. RESULTS AND DISCUSSION

3.1. X-ray diffraction

X-ray powder diffraction patterns for pure host [Ag_2CdI_4], and doped samples of [$xCuI:(1-x)Ag_2CdI_4$], recorded at room temperature are shown in Fig. 1(a) and 1(b), at room temperature. The x-ray diffractogram values of all the composite samples [$xCuI:(1-x)Ag_2CdI_4$], correspond to standard values of [Ag_2CdI_4] and careful analysis revealed that in addition to standard peaks of pure host [Ag_2CdI_4], a number of peaks appeared for the Cu^+ doped host composite system.

The appearance of seven tiny peaks (reflections at 13.04°, 24.82°, 40.41°, 48.05°, 58.24°, 64.29°, 73.52°) observed in x=0.2 CuI -doped composite, shifted to (13.04°, 24.65°, 41.03°, 48.40°, 59.39°, 65.31°, 74.47), (13.04°, 25.28°, 41.52°, 49.35°, 60.34°, 66.59°, 76.06) and (12.72°, 25.28°, 41.83°, 49.67°, 60.66°, 66.91°, 76.38°) in the x=0.4, 0.6 and x=0.8 mol. wt.% CuI -doped composite systems, respectively, and the corresponding peaks were more intense upon doping.

The findings indicate a significant structural change with only small compositional changes [23] in the host composite system [Ag_2CdI_4], with a gradual increase in CuI respectively. It is therefore concluded that the phase composition is influenced by the presence of the dopant [22,24].
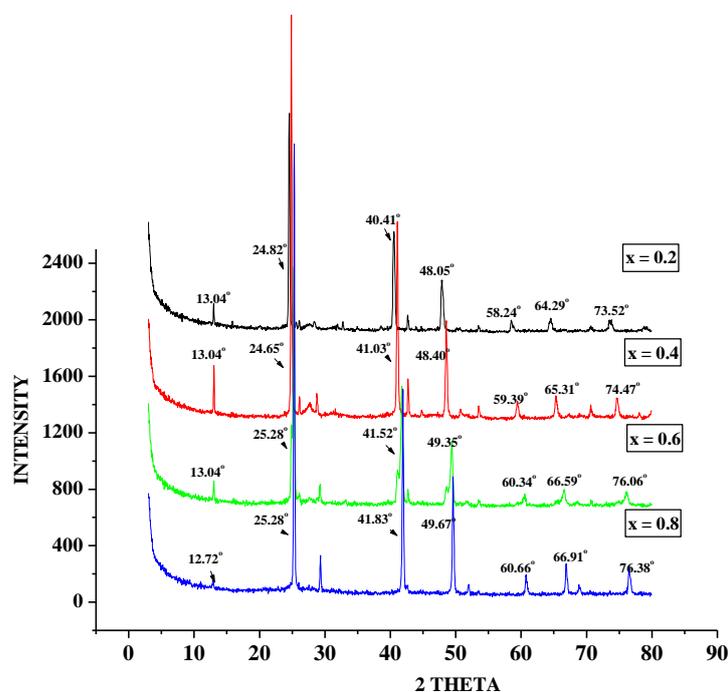

Fig. 1. X-ray diffractogram for [$xCuI.(1-x)Ag_2CdI_4$] fast ion conductors, where (x=0.2,0.4, 0.6 and 0.8 mol. wt.%)

3.2. FTIR analysis

Infrared transmission spectra of the fast ionic conductors [$xCuI:(1-x)Ag_2CdI_4$] where (x=0.2, 0.4, 0.6 and 0.8 mol. wt.%) have been measured in the mid-infrared range (400-4000 cm^{-1}) to investigate the structure of the iodine anion matrix and the nature of sited hosting the charge carrier copper ions [25]. Vibrations of the local polyhedra of electrolytes forming cations give rise to intense bands observed mainly in the mid-infrared range. The nature of the coordination environments of the electrolytes modifying cations, i.e. Cu$^+$, can be deduced

from the analysis of the localized cation motion active in the far infrared [26,27]. Infrared measurements can provide information on the motion of mobile ions and environment of the ions. Fig. 2, shows the far-IR transmission spectrum of [$xCuI$:$(1-x)Ag_2CdI_4$] fast ionic conductors at room temperature, there are six distinct bands at 427, 449, 470 , 493 , 520 and 1601 cm^{-1} in pure Ag_2CdI_4. Ag_2CdI_4 has the tetragonal structure [19] at room temperature, the same as that of Ag_2HgI_4 and Cu_2HgI_4 compounds [28]. Shriver et al. [28] have calculated the vibrational modes (using factor group analysis) as 3A + 5B + 5E. Hence the vibrational modes of Ag_2CdI_4 is 3A + 5B + 5E. Only B and E models are IR active.

According to Factor group analysis, there should be 13 modes for Ag_2CdI_4 at low temperatures [29]. The vibrational modes can be assigned by considering Ag_2CdI_4 as consisting o f the vibrational modes of AgI and $(CdI_4)^{2-}$ species. In fact, as shown in Fig. 2, almost all the bands due to AgI and $(CdI_4)^{2-}$ are seen in the pure Ag_2CdI_4 composites. The band at 1601 cm^{-1} can be assigned to the symmetric stretching "A" mode of $(CdI_4)^{2-}$ species and this band is the strongest band at room temperature. This assignment is in good agreement with the other $(CdI_4)^{2-}$ tetrahedral compound s [30]. On the doping of 0.2 Cu^+ ions in the pure Ag_2CdI_4 all six bands shifted to 441, 477, 528, 668, 1244, 1463 and 1610 cm^{-1}. The 1000 - 1500 cm^{-1} region consists o f two bands at the positions 1244 cm^{-1} and 1463 cm^{-1} at room temperature and at low temperature, these bands are expected to split. It is known from the IR spectra of x=0.2 Cu^+ ion conductors that this region consists of mostly CuI [31] stretching modes. Hence, in all [$xCuI$:$(1-x)Ag_2CdI_4$] composite samples, also the bands in this region can be assigned to symmetric stretching modes of CuI. Below 700 cm^{-1}, there are five sharp bands at 427, 449, 470, 493 and 520 cm^{-1} in pure Ag_2CdI_4 and four sharp bands at 668, 528, 477 and 441 cm^{-1}, 695, 509, 469 and 429 cm^{-1}, 612, 532, 477 and 437 cm^{-1} and five bands at 664, 612, 548, 497 and 433 cm^{-1} in x = 0.2, 0.4, 0.6 and 0.8 Cu^+ ions conductors respectively, it is known from earlier studies [32] that the bands in this region are due to deformation type metal-iodine vibrations. On comparison with $(CdI_4)^{2-}$ species vibrations, the bands at 520 and 493 cm^{-1} in pure Ag_2CdI_4, and 668 cm^{-1} and 528 cm^{-1}, 695 and 509 cm^{-1}, 612 and 532 cm^{-1} and 664 and 612 cm^{-1} in x=0.2, 0.4, 0.6 and 0.8 Cu^+-ions conductors respectively, can be assigned to Cd - I deformation type bands. The band at 470 cm^{-1} in pure Ag_2CdI_4, and 477, 469, 477 and 548 cm^{-1} in x=0.2, 0.4, 0.6 and 0.8 mol. wt.% Cu^+- doped ions conductors respectively, is attributed to the E symmetry of Ag^+ translational mode and is the characteristic attempt frequency of Ag^+ ion arising from the diffusive behavior to oscillatory behavior. This assignment is well explained by Shriver [33] by referring to the negative pressure dependence and also using theoretical calculations.
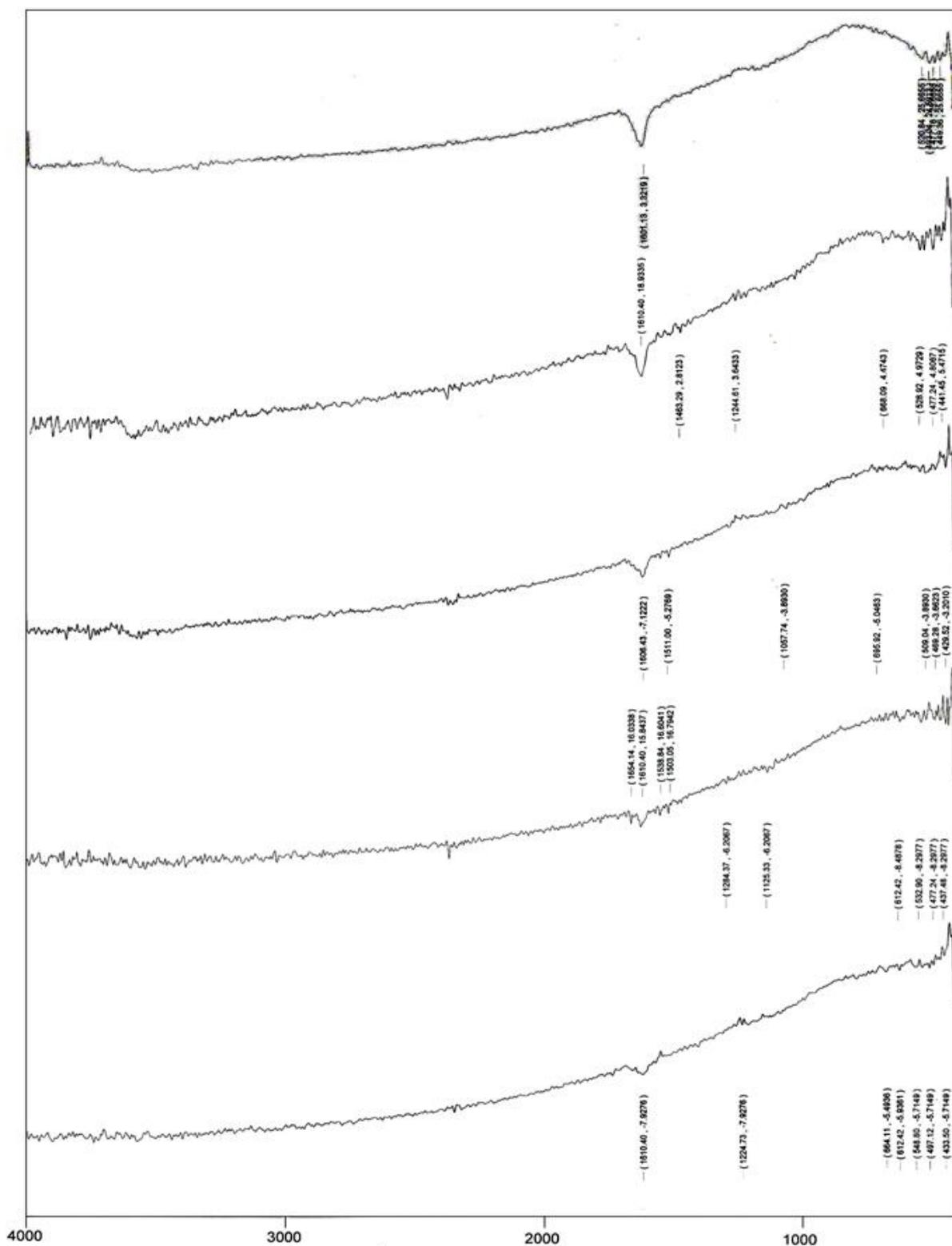
Fig. 2. FTIR spectrum pure Ag_2CdI_4 and for $[xCuI:(1-x)Ag_2CdI_4]$ fast ion conductors, where (x = 0.2,0.4, 0.6 and 0.8 mol. wt.%)

Table 2. Ag_2CdI_4 and $[xCuI:(1-x)Ag_2CdI_4]$ fast ion conductors, where (x=0.2,0.4, 0.6 and 0.8 mol. wt.%), room temperature peaks and assignment

Far-IR transmission					Assignment
Pure Ag_2CdI_4	$CuI_{(0.2)}$: $(Ag_2CdI_4)_{(0.8)}$	$CuI_{(0.4)}$: $(Ag_2CdI_4)_{(0.6)}$	$CuI_{(0.6)}$: $(Ag_2CdI_4)_{(0.4)}$	$CuI_{(0.8)}$: $(Ag_2CdI_4)_{(0.2)}$	
470.20	477.24	469.28	477.24	548.80	
449.36	441.45	429.52	437.48	497.12	Ag-I deformation
427.61	----	----	----	433.50	
520.84	668.09	695.92	612.42	664.11	Cd-I deformation
493.04	528.92	509.04	532.92	612.42	
----	1463.29	1511.00	1284.37	1224.73	Cu-I
----	1244.61	1057.74	1125.33	----	symmetric stretch
----	----	----	1538.84	----	Ag-I
----	----	----	1503.05	----	symmetric stretch
1601.13	1610.40	1606.43	1654.14	1610.40	$(CdI_4)^{2-}$- I
----	----	----	1610.40	----	symmetric stretch

The value assigned to the attempt frequencies in Ag_2CdI_4 is similar to cation transition modes in other related Cu^+-doped fast ionic conductors [33]. Another possibility is that motion of very large amplitude (diffusive like) is able to create configurational disorder which allows all IR modes [29].

Inspection of Table 1 and Fig. 2, shows that IR spectra of the x = 0.2 and 0.4 mol. wt.% conductors exhibit the strongest feature at ca 1610.40 cm^{-1} and 1606.42 cm^{-1} respectively, while the infrared activity below 900 cm^{-1} is weak. On the basis of the above discussion, these results strongly suggest that the existence of $(CdI_4)_2^{2-}$/ $2Cu^+$ tetrahedral in the x = 0.2 and 0.4 mol. wt.% fast ionic conductors should be excluded at least in concentration detectable by infrared spectroscopy.

Therefore, it is found that the infrared activity of the x=0.2 and x=0.4 mol. wt.% fast ionic conductors arises from $(CdI_4)^{2-}$ tetrahedral, while x=0.6 and x=0.8 mol. wt.% fast ionic

conductors show weakest feature at higher and lower frequencies. Increasing the CuI content induces a decrease of the infrared activity.

3.3. Thermal analysis

3.3.1. Differantial thermal analysis

DTA curves for [xCuI:(1-x)Ag$_2$CdI$_4$], are shown in Fig. 3. All the DTA curves contained three endothermic peaks, the first endotherm attributed to interface interactions between CuI and [Ag$_2$CdI$_4$] [34], second endotherm corresponded to a β–α transition (≈176.53°C for [Ag$_2$CdI$_4$]) and the third endotherm corresponded to melting of the material [35]. It is observed that, in [xCuI:(1-x)Ag$_2$CdI$_4$], composite samples, the melting point of pure sample is 499.96°C, which thereafter decreases to increases as 435°C, 440°C in, 0.2 and 0.4 mol. wt.% while in 0.6 and 0.8 mol. wt.% CuI doped sample the melting point again decreases to increases as 330°C, 360°C respectively with increasing CuI concentration in host sample.
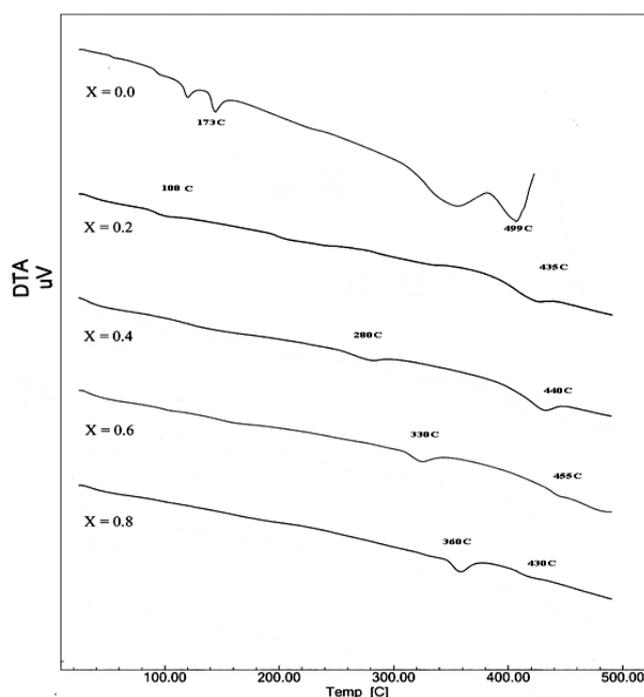

Fig. 3. Differential thermal analysis (DTA) curves for mixed composite systems [xCuI.(1-x)Ag$_2$CdI$_4$] where (x = 0.2, 0.4, 0.6,0.8 mol. wt.%)

It is observed that, in [xCuI:(1-x) Ag$_2$CdI$_4$], composite samples, the melting point of pure sample is 499.96°C, which thereafter decreases to increases as 435°C, 440°C in, 0.2 and 0.4 mol. wt.% while in 0.6 and 0.8 mol. wt.% CuI doped sample the melting point again decreases to increases as 330°C, 360°C respectively, with increasing CuI concentration in host sample. There is clear evidence that the transition temperature shifted to higher

temperature as 0.4 mol. wt.% Cu^+ dopant concentration increases. This indicate the significant interaction between host [xCuI:(1-x)Ag_2CdI_4], system with dopant CuI content.

3.3.2. Differential scanning calorimetry

Fig. 4 shows the heating mode of DSC curves of all the [xCuI:(1-x)Ag_2CdI_4], composite samples taken in the temperature range 30–500°C. In the [Ag_2CdI_4] samples, shows the expected behavior with moderate strength peak when it appeared at 176.81°C, which corresponds to β–α phase transition of the compound [34], and intensive peak at 462.74°C, which is attributed to melting point. β–α phase transition peak becomes broad with CuI content; this is due to the form of crystalline phase within space charge layer that is expected to form between CuI and [Ag_2CdI_4]. Melting peak of 0.2 mol. wt % CuI has a large hump at about 451.11°C on the low-temperature side of the melting peak, which slightly shifts toward higher temperature side 472.96°C with increase in 0.4 mol. wt % CuI content, in 0.6 samples it shifts toward lower temperature side at about 452.32°C.
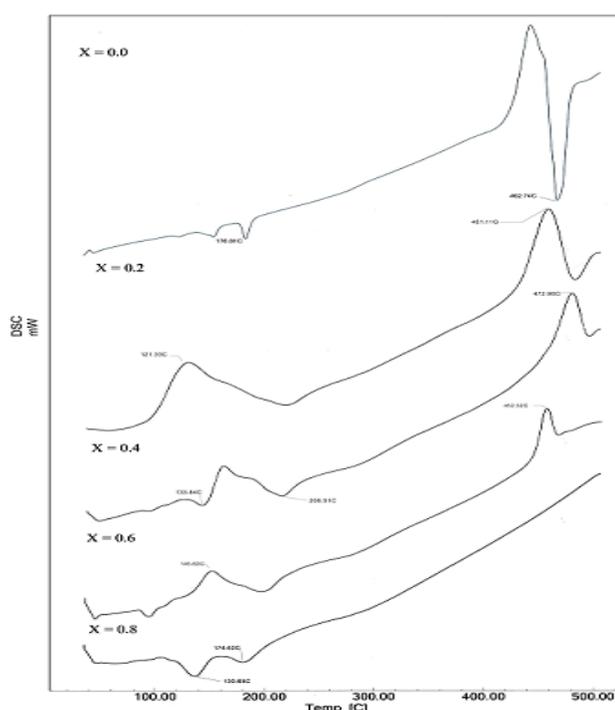

Fig. 4. Differential scanning calorimetry (DSC) curves for mixed composite systems [xCuI:(1-x)Ag_2CdI_4], where (x = 0.2,0.4,0.6 and 0.8 mol. wt.%)

While on further increase in (0.8 mol. wt %) CuI^- content to the pure host, the melting peak shifts towards far lower temperature side at about 174.64°C. It has been observed from the DSC curve that an additional peak is obtained before the β–α phase transition peak with the addition of CuI and its intensity increase with the mole fraction of copper iodide. This peak attributed to interface interactions between CuI and [Ag_2CdI_4].

The mixture samples show no appreciable effect on the temperature of the phase transition: $RbNO_3$–Al_2O_3 [36], $CsCl$–Al_2O_3 [37], and $Cs_2H_3(SO_4)_4$–SiO_2 [38]. This behavior has been observed frequently in the ionic salt oxide composite such as that noticed with an increase in alumina content, the formation of the composite

3.3.3. Thermogravimetric analysis

Phase transition of all the composites were studied by thermogravimetric analysis in the temperature range 20-400°C [Fig. 5].
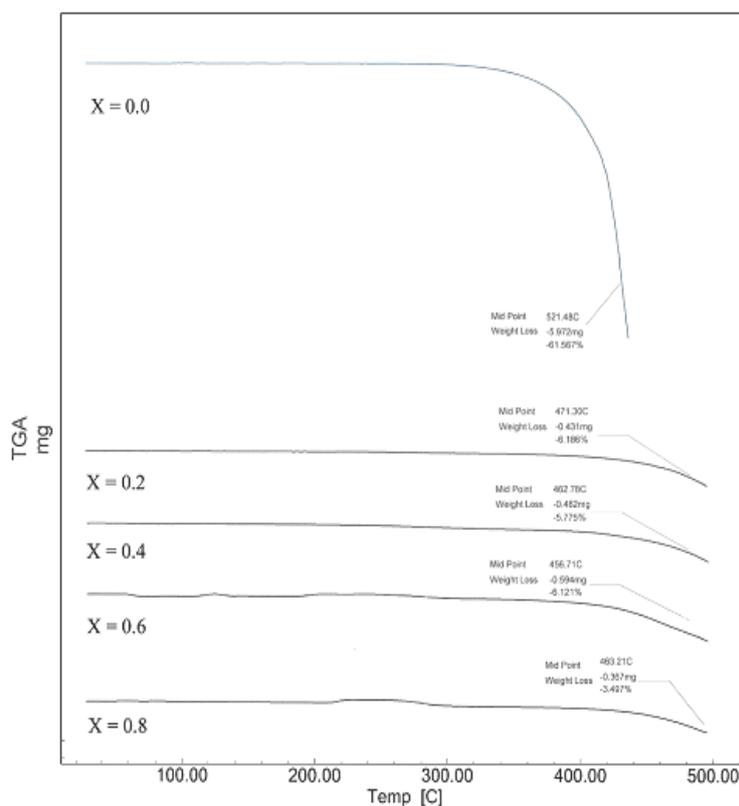

Fig. 5. Thermogravimetric analysis (TGA) curves for mixed composite systems [xCuI:(1-x)Ag_2CdI_4], where (x=0.2, 0.4, 0.6 and 0.8 mol. wt.%)

In the TGA curves of [xCuI:(1-x)Ag_2CdI_4], [Fig. 5], from room temperature up to about 400 °C. One distinct peak of TGA are obtained for the [xCuI.(1-x)Ag_2CdI_4], in the temperature range 400–500°C with corresponding mass loss of 5.927 mg for pure samples, 0.431 mg for 0.2 CuI mol. wt. %, 0.482 mg for 0.4 CuI mol. wt. %, 0.594 mg 0.6 CuI mol. wt. %, and -0.367 mg for 0.8 CuI mol. wt.% [39]. These data corroborate the observations of TGA studies.

4. CONCLUSION

A novel composite superionic systems [xCuI.(1-x)Ag$_2$CdI$_4$], were investigated. In the host [Ag$_2$CdI$_4$] structure, doping with Cu$^+$ in the host induces a decrease in the mobile charge carriers, Ag$^+$ ions that is proportionate with the increased 0.x mol. wt.% in the host mixed system.

X-ray powder diffraction, FTIR, DTA, DSC and TGA studies confirmed the formation of a superionic phase in the composite system. The temperature dependence of various ionic parameters was determined to characterize the ion transport properties and doping effect.

REFERENCES

[1]   A. Viswanathan, and S. A. Suthanthiraj, Solid State Ion 58 (1992) 89.

[2]   K. Siraj, and R. Rafiuddin, Soft Nanosci. Lett. 2 (2012) 13.

[3]   I. M. Bolesta, O.V. Futey, and O. G. Syrbu, Solid State Ion 119 (1999) 103.

[4]   C. P. Varsamis, E. I. Kamitsos, N. Machida, and T. Minami, J. Phys. Chem. B 101 (1997) 3734.

[5]   T. Tsurui, J. Kawamura, and K. Suzuki, J. Non. Cryst. Solid 353 (2007) 302.

[6]   T. Minami, and N. Machida, Mater. Chem. Phys. 23 (1989) 63.

[7]   A. Viswanathan, and S. A. Suthanthiraj, Solid State Ion 62 (1993) 79.

[8]   B. V. R. Chowdhari, K. L.Tan, and F. Ling, Solid State Ion 107 (1998) 89.

[9]   A. Viswanathan, and S. A. Suthanthiraj, Solid State Ion 62 (1993) 79.

[10] R. G. Pearson, J. Chem. Education. 45 (1968) 581.

[11] R. F. Bartholomew, W. G. Porfield, J. A. Murphy, J. E. Pierson, S. D. Stooky and P. A. Tick, US Pat. 4, 226, (1980) 628.

[12] T. Minami, J. Non.Cryst. Solids 173 (1985) 273.

[13] R. Sudharsanan, Solid State Ion 9-10 (1982) 1473.

[14] R. Sudarsanan, T. K. K. Srinivasan, and S. Radhakrishna, Solis State Ion 13 (1984) 277-283.

[15] I. Bolesta, O. Futey, and S. Velgosh, Ukrain. J. Phys. Optic. 1 (2000) 13.

[16] O. N. Yunakova, V. K. Miloslavski, and E. N. Kovalenko, Phys. Solid State 43 (2001) 1072.

[17] S. M. Nair, and A. Ahmad, J. Phy. Chem. Sol. 58 (1997) 331-333.

[18] T. Matsui, and J. B. Wagner, Jr., J. Electrochem. Soc. 124 (1977) 937.

[19] J. Otsubo, A. Nitta, M. Kaneka, Y. Iwata, and A. Ueki, J. Chem. Soc. Japan 69 (1966) 1718.

[20] Noorussaba, and A. Ahmad, Anal. Bioanal. Electrochem. 3 (2011) 521.

[21] Noorussaba, and A. Ahmad, Bull. Mater. Sci. 33 (2010) 419.

[22] Noorussaba, and A. Ahmad, Cen. Europ. J. Chem. 8 (2010) 1227.

[23] S. Ya, I. Stomin, S. V. Chernov, E. V. Antipov, S. Yu, and A. Dobrovolsky, Sol. Stat. Chem. 180 (2007) 1882.

[24] A. Adamski, Z. Sojka, K. Dyrek, and M. Che, Sol. Stat. Ion 117 (1999) 113.

[25] C. P. Varsamis, and E. I. Kamitsos, J. Phys. Chem. B 101 (1997) 3734.

[26] E. I. Kamitsos, A. P. Patsis, M. A. Karakassides, and G. D. Chryssikos, J. Non.Cryst. Solid 126 (1990) 52.

[27] E. I. Kamitsos, A. P. Patsis, and G. D. Chryssikos, J. Non-Cryst. Solid. 152 (1993) 246.

[28] D. R. Greig, G. C. Joy, and D. F. Shriver, J. Chem. Phys. 67 (1977) 3189.

[29] R. Sudharsanan, T. K. K. Srinivasan, and S. Radhakrishna, Solid State Ion 13 (1984) 277.

[30] J. E. D. Davies, and D. A. Long, J. Chem. Soc. A. (1968) 2054.

[31] G. L. Bottger, and A. L. Gedded, J. Chem. Phys. 57 (1972) 1215.

[32] D. R. Greig, and D. G. Shriver, J. Chem. Phys. 66 (1976) 5248.

[33] J. I. Mcomber, and D. F. Shriver, J. Phys. Chem. Solid. 43 (1982) 895.

[34] S. Sultana, and R. Rafiuddin, Ionics 15 (2009) 621.

[35] R.C. Agrawal, and R. Kumar, J. Phys. D: Appl. Phys. 27 (1994) 2431.

[36] N. F. Uvarov, P. Vanek, Yu. I. Yuzyuk, V. Zelezný, V. Studnicka, B. B. Bokhonov, V. E. Dulepov, and J. Petzelt, Sol. Stat. Ion 90 (1996) 201.

[37] N. F. Uvarov, B. B. Bokhonov, V. P. Isupov, and E. F. Hairetdinov, Sol. Stat. Ion 74 (1994) 15.

[38] G. V. Lavrova, V. G. Ponomareva, and E. B. Burgina, Sol. Stat. Ion 176 (2005) 767-771.

[39] A. Phukan, J. N. Ganguli, and D. K. Dutta, J. Mol. Catal. A: Chem. 202 (2003) 279.